

Events with Isolated Charged Leptons and Large Missing Transverse Momentum at HERA

Tancredi Carli

CERN, Experimental Physics Division, CH-1211 Geneva 23, Switzerland
Tancredi.Carli@cern.ch

Dominik Dannheim

DESY, Notkestr. 85, D-22607 Hamburg
Dominik.Dannheim@desy.de

Lorenzo Bellagamba

INFN, Dipartimento di Fisica, via Irnerio 46, I-40126 Bologna
Lorenzo.Bellagamba@bo.infn.it

Striking events with isolated charged leptons, large missing transverse momentum and large transverse momentum of the hadronic final state (P_T^X) were observed at the electron proton collider HERA in a data sample corresponding to an integrated luminosity of about 130 pb^{-1} . The H1 collaboration observed 11 events with isolated electrons or muons and with $P_T^X > 25 \text{ GeV}$. Only 3.4 ± 0.6 events were expected from Standard Model (SM) processes. Six of these events have $P_T^X > 40 \text{ GeV}$, while 1.3 ± 0.3 events were expected. The ZEUS collaboration observed good agreement with the SM. However, ZEUS found two events with a similar event topology, but tau leptons instead of electrons or muons in the final state. Only 0.2 ± 0.05 events were expected from SM processes. For various hypotheses the compatibility of the experimental results was investigated with respect to the SM and with respect to possible explanations beyond the SM. Prospects for the high-luminosity HERA-II data taking period are given.

Keywords: Searches beyond the Standard Model, HERA, tau leptons

1. Introduction

The Standard $SU(3) \otimes SU(2) \otimes U(1)$ Model (SM) of particle physics describes the electroweak and strong interactions between elementary particles in both the low- and the high-energy regime to an amazing accuracy. It is, however, unsatisfactory in the sense that many fundamental facts such as the quark-lepton symmetry, the structure of the gauge groups and the spectrum of the particle masses remain unexplained. Furthermore, the inclusion of gravitation as the fourth fundamental force in nature remains an open question. Recently, hints for the need of an extension of the SM were obtained by the observation of neutrino oscillations suggesting a flavour mixing also in the leptonic sector and non-zero neutrino rest masses¹. Only future experiments will be able to fully clarify the nature of this phenomenon. Anyway, a crucial step forward, towards a deeper understanding of the fundamental particles

and their interactions, would be the experimental observation of new heavy particles beyond the presently known particle spectrum.

The high centre-of-mass energy, \sqrt{s} , of HERA colliding positrons of energy $E_e = 27.5$ GeV with protons of energy $E_p = 920$ GeV offers the possibility to directly produce new heavy particles with a mass up to $\sqrt{s} = 318$ GeV^a. In addition, new heavy particles can also interfere, via virtual effects, with SM processes, resulting in an enhancement or deficit in measured cross sections over the SM expectation. HERA is hence also sensitive to particles with masses higher than the centre-of-mass energy.

Searches for new particles and new interactions beyond the SM (BSM) at HERA were reviewed recently². Here, the final HERA-I results^{3,4,5,6,7} on the search for events with isolated charged leptons (l : electron, muon or tau lepton), with large missing transverse momentum (P_T^{miss}) and with large transverse momentum of the hadronic final state (P_T^X), $ep \rightarrow l\nu X$, are reviewed. Such an event signature is typical for a singly produced heavy particle decaying into a charged lepton and a neutrino. The possibility to produce BSM particles leading to this signature has been extensively discussed^{8,9,10}.

2. Calculation of the SM Process $ep \rightarrow eW^\pm X$

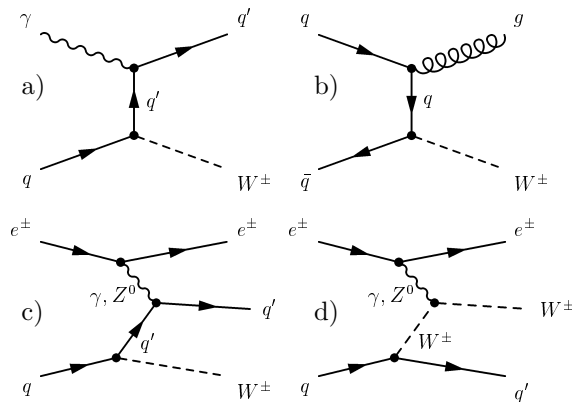


Fig. 1. Examples of leading order Feynman diagrams for W^\pm -boson production at HERA through direct (a) and resolved (b) photoproduction, the DIS process (c) and triple gauge boson coupling (d).

production at HERA are shown in Fig. 1. The first two diagrams represent collisions of real photons with protons (photoproduction). In Fig. 1a the photon inter-

Within the SM the dominant process leading to isolated charged leptons and large P_T^{miss} is the production of W^\pm -bosons ($ep \rightarrow eW^\pm X$). This process has a small cross section. The inclusive W^\pm -boson production cross section is $\sigma(ep \rightarrow eW^\pm X) \approx 1$ pb. However, in this process the transverse momentum of the hadronic final state P_T^X is expected to be relatively small. If $P_T^X > 25$ GeV is required, the cross section drops to approximately 0.2 pb.

Typical leading order Feynman diagrams of W^\pm -boson

^aIn the data taking period 1994-1997 the proton energy was 820 GeV ($\sqrt{s} = 300$ GeV). This period corresponds to an integrated luminosity of 37 pb^{-1} (48 pb^{-1}) for H1 (ZEUS). In 1998/1999 HERA collided electrons on protons, corresponding to an integrated luminosity of approximately 14 pb^{-1} (17 pb^{-1}) for H1 (ZEUS).

acts directly as point-like particle $\gamma q \rightarrow qW^\pm$ (direct photoproduction), in Fig. 1b it splits into a quark anti-quark pair before interacting with the hard subprocess $qq \rightarrow gW^\pm$ (resolved photoproduction). Figure 1c shows the deep-inelastic scattering (DIS) process $\gamma^*q \rightarrow qW^\pm$, where the photon is virtual. If the photon virtuality is high ($Q^2 \gg 1 \text{ GeV}^2$), the scattered electron can be measured in the main detector. In each of these diagrams, the W^\pm -boson is radiated from a quark in the proton. This is the dominant single contribution of in total seven contributing diagrams. Of particular interest is the diagram where the interaction proceeds via the triple gauge boson coupling ($\gamma W^\pm W^\pm$, see Fig. 1d). This process allows the anomalous trilinear coupling of gauge bosons to be tested at HERA¹¹. However, limits on an anomalous triple boson coupling obtained on part of the data set by ZEUS⁵ are not competitive with the precise data from LEP¹² and Tevatron¹³.

The direct photoproduction process gives the dominant contribution to the total cross section. The DIS contribution is about a factor of two smaller. The resolved photoproduction process is negligible at high transverse momenta. The process $ep \rightarrow \nu W^\pm X$ contributes about 5% and can thus be neglected.

The leading order (LO) $\mathcal{O}(\alpha^2)$ calculation and Monte Carlo (MC) simulation of the $ep \rightarrow eW^\pm X$ process has been available since the start-up of HERA^{14,15}. Recently, the $\mathcal{O}(\alpha^2\alpha_s)$ QCD corrections were calculated for the dominant direct photoproduction contribution¹⁶. They include the virtual corrections due to one-loop diagrams generated by virtual gluon exchange and the real corrections due to gluon radiation from the quark lines. In the calculation, the renormalisation and factorisation scales were set to $\mu^2 = M_W^2$, where M_W is the mass of the W^\pm -boson. The QCD corrections modify the LO result by (10 – 15%) and reduce the dependence of the calculated cross section on μ from about 20% to about 5%^b. For the analyses reviewed here, a reweighting method for the LO W^\pm -production MC simulations was used¹⁷, which takes into account the QCD corrections and reduces the uncertainty on the cross section to approximately 10-15%.

3. Observation of Events with Isolated Electrons or Muons

Events were selected by requiring large P_T^{miss} and an electron (e) or muon (μ) with high transverse momentum (P_T^l) in the acceptance of the detector. The lepton (l) had to be isolated, i.e. the distance in the $\eta - \phi$ plane^c from the axis of the closest jet $D_{\text{jet}} = \sqrt{\Delta\eta_{l\text{jet}}^2 + \Delta\phi_{l\text{jet}}^2}$ and the distance from the nearest track $D_{\text{trk}} = \sqrt{\Delta\eta_{l\text{trk}}^2 + \Delta\phi_{l\text{trk}}^2}$ had to be large. Jets were defined by the inclusive longitudinally invariant k_T clustering algorithm¹⁸ and were required to have a transverse energy $E_T > 5 \text{ GeV}$. ZEUS required in addition $-1 < \eta_{\text{jet}} < 2.5$. In the electron channel,

^bThe residual scale dependence is evaluated by varying μ in the range $4\mu^2 - 0.25\mu^2$.

^cThe variable η denotes the pseudo-rapidity defined by $\eta = -\ln \tan(\theta/2)$, where θ is the polar angle measured with respect to the proton-beam direction. The variable ϕ denotes the azimuthal angle.

4 *T. Carli, D. Dannheim, L. Bellagamba*

H1 applied the cut on D_{trk} only for electron polar angles bigger than 45° .

To efficiently remove neutral current (NC) DIS, events with a back-to-back topology in the azimuthal plane were rejected by a cut on the difference between the direction of the lepton and the hadronic final state momentum $\Delta\Phi_{lX}$. Different cut values were applied for the electron and muon channel. Furthermore a cut on the longitudinal momentum balance δ_{miss} was applied^d.

To gain sensitivity at low P_T^{miss} , H1 used the ratio $V_{\text{ap}}/V_{\text{p}}$ of the anti-parallel to parallel components of the measured calorimetric transverse momentum, with respect to the direction of the calorimetric transverse momentum. This variable measures the azimuthal balance of the event. Events with high- p_T particles that do not deposit much energy in the calorimeter (μ, ν) generally have low values of $V_{\text{ap}}/V_{\text{p}}$. In addition, in the electron channel the reconstructed squared momentum transfer $\xi_e^2 = 4E'_e E_e \cos\theta_e/2 > 5000 \text{ GeV}^2$ was used for $P_T^X < 25 \text{ GeV}$, where E'_e is the energy and θ_e the polar angle of the isolated electron. This observable corresponds to the photon virtuality Q^2 , if the scattered electron in a NC DIS process is measured. Since the NC DIS cross section falls steeply with Q^2 , ξ_e^2 is generally lower in NC DIS than in W^\pm -boson production.

Table 1. Main H1 and ZEUS event selection cuts for events with isolated electrons (e) or muons (μ). Some of the cuts are only applied in the e or μ channel.

H1	ZEUS
$5^\circ < \theta_l < 140^\circ$	$17^\circ \lesssim \theta_l < 115^\circ$
$P_T^l > 10 \text{ GeV}$	$P_T^l > 5 \text{ GeV}$
$P_T^{\text{miss}} > 12 \text{ GeV}$	$P_T^{\text{miss}} > 20 \text{ GeV}$
$D_{\text{jet}} > 1.0$	$D_{\text{jet}} > 1.0$
$D_{\text{trk}} > 0.5$ for $\theta_e > 45^\circ$ (e)	$D_{\text{trk}} > 0.5$
$D_{\text{trk}} > 0.5$ (μ)	
$\Delta\phi_{lX} < 160^\circ$ (e), 170° (μ)	$\Delta\phi_{lX} < 172^\circ$ (e)
$\delta_{\text{miss}} > 5 \text{ GeV}$	$\delta_{\text{miss}} > 8 \text{ GeV}$ (e)
$V_{\text{ap}}/V_{\text{p}} < 0.5$ (e)	
$\xi_e^2 > 5000 \text{ GeV}^2$ (e)	

The most important selection criteria for the H1 and ZEUS analyses are summarised in Tab. 1. The main differences are the requirements on P_T^{miss} and the lepton acceptance.

These selection criteria were designed to reject the main background processes with high cross sections, i.e. mismeasured NC, $ep \rightarrow eX$, and charged current (CC), $ep \rightarrow \nu X$, DIS events, two-jet-photoproduction

events, $ep \rightarrow \text{jet jet } X$, and events where two leptons are produced in inelastic photon-photon collisions, $ep \rightarrow e l^+ l^- X$. The H1 event selection has been optimised to increase the acceptance for W^\pm -boson production, resulting in a selection efficiency of 40% for $ep \rightarrow W^\pm X$ events with $P_T^X > 25 \text{ GeV}$. The ZEUS event selection was more oriented towards the search for a singly produced heavy particle and was less efficient for W^\pm -boson production.

H1 observed 11 events in the electron channel and 8 events in the muon channel. Most of these events were found in the e^+p data taking period corresponding to $\int \mathcal{L} dt \approx 105 \text{ pb}^{-1}$. In the e^-p data, which are a fraction of about 10% of the total

^dThe variable δ_{miss} is defined as $\delta_{\text{miss}} = 2E_e - \sum_i E_i(1 - \cos\theta_i)$, where E_i and θ_i denote the energy and the polar angle of each energy deposit, respectively, and E_e is the electron beam energy. For an event where only momentum in the proton-beam direction is undetected, $\delta_{\text{miss}} = 0$.

Table 2. Number of measured and expected events in the H1 and ZEUS analyses of events with isolated electrons or muons, large P_T^{miss} and large P_T^X . Both, the number of events expected from all SM processes and the contribution from the $ep \rightarrow eW^\pm X$ process in percent are given.

H1	$P_T^X > 25 \text{ GeV}$			$P_T^X > 40 \text{ GeV}$		
	Data	SM	$W^\pm\text{-contr.}$	Data	SM	$W^\pm\text{-contr.}$
electron	5	1.8 ± 0.3	82%	3	0.7 ± 0.1	80%
muon	6	1.7 ± 0.3	88%	3	0.6 ± 0.1	92%
combined	11	3.4 ± 0.6	85%	6	1.3 ± 0.3	86%
ZEUS	Data	SM	W-contr.	Data	SM	W-contr.
electron	2	$2.9^{+0.6}_{-0.3}$	45%	0	0.9 ± 0.1	61%
muon	5	2.8 ± 0.2	50%	0	1.0 ± 0.1	61%
combined	7	5.7 ± 0.6	47%	0	1.9 ± 0.2	61%

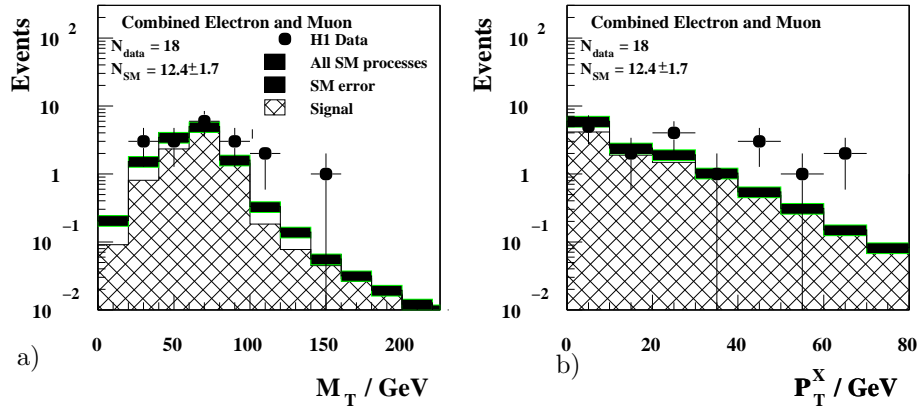


Fig. 2. The transverse mass (a) and transverse momentum of the hadronic final state (b) distribution for the H1 events with isolated electrons or muons and missing transverse momentum in the e^+p data sample ($\int \mathcal{L} dt \approx 105 \text{ pb}^{-1}$). The open histogram indicates the expectation for SM processes, the shaded band the total uncertainty. The hatched histogram indicates the contribution from W^\pm -boson production. The total number of observed data events (N_{data}) and the total number of expected SM events (N_{SM}) is also given.

data sample, only one electron event was found. In the electron (muon) channel 11.5 ± 1.5 (2.9 ± 0.5) events were expected from SM processes, 71% (86%) from $e^\pm p \rightarrow W^\pm X$.

The transverse-mass (M_T) distribution of the electron or muon and the neutrino reconstructed from the missing momentum (see Fig. 2a) is compatible with the distribution expected from a W^\pm -decay and agrees with the SM expectation. The striking feature of these events, however, is their large P_T^X . While for low P_T^X the number of measured events roughly corresponded to the number of expected events, an excess of data events was seen towards large P_T^X (see Fig. 2b). The number of measured and expected events with electrons or muons and with $P_T^X > 25 \text{ GeV}$ or $P_T^X > 40 \text{ GeV}$ are summarised in Tab. 2. An additional prominent event^{19,20,21}, where a scattered muon balances the transverse momentum of the hadronic system, was rejected by the cut on $\Delta\phi_{lX}$.

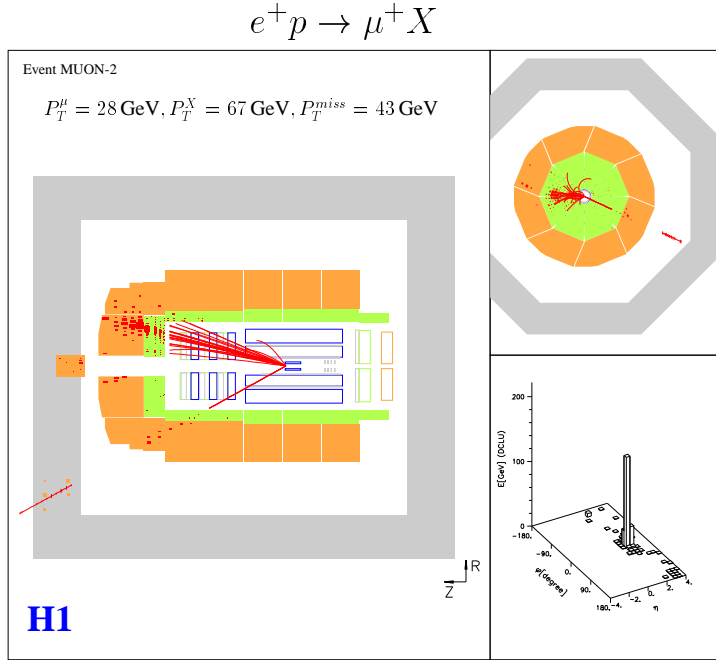
6 *T. Carli, D. Dannheim, L. Bellagamba*

Fig. 3. Display of an isolated muon event with large P_T^{miss} and large P_T^X in the H1 detector.

In the electron channel with $P_T^X > 25$ GeV, four events had a clearly identified positron (e^+), in one event the charge could not be measured. In the muon channel three events had a μ^+ and two a μ^- . For the remaining event the charge could not be determined with sufficient accuracy. One of the muon events is shown in Fig. 3.

In the combined electron and muon channel, H1 observed 6 events with $P_T^X > 40$ GeV, while only 1.3 ± 0.3 events were expected from SM processes. The Poisson probability for the SM expectation to fluctuate to this observed number of events or more is about 0.3%.

The ZEUS data were consistent with the expected SM background in all kinematic regions. In the electron (muon) channel 24 (12) events were observed, while $20.6^{+1.7}_{-4.6}$ ($11.9^{+0.6}_{-0.7}$) events were expected from SM processes. For $P_T^X > 25$ GeV, 7 events were found and 5.7 ± 0.6 were expected from SM processes. No event with $P_T^X > 40$ GeV was observed, while 1.9 ± 0.2 events were expected. The excess reported by H1 was thus not confirmed by ZEUS.

4. Observation of Events with Isolated Tau Leptons

The ZEUS collaboration also extended the search to events with isolated tau leptons, large P_T^{miss} and large P_T^X .

4.1. Tau-Lepton Identification

The tau-leptons were identified in their hadronic decay mode. In contrast to jets initiated by quarks or gluons, jets produced by tau-leptons are pencil-like, collimated and have a low charged-particle multiplicity. The tau-lepton identification was developed using independent event samples^e.

The main background process is CC DIS where a jet from the hadronic final state is misidentified as tau lepton. The CC DIS cross section is about three orders of magnitude higher than the signal from W^\pm -boson production followed by a $W \rightarrow \tau\nu_\tau$ decay. To strongly suppress this large background while keeping a sufficiently large detection efficiency for the tau leptons, a multi-variate discrimination technique, called PDE-RS^f, was used²³. Six observables were exploited to characterise the internal jet structure^g: the first and second moment of the radial extension of the jet^h, the first and second moment of the projection of the jet onto its axis, the subjet multiplicityⁱ and the invariant mass of the jet four-vector, calculated from the calorimeter cells associated to the jet. The classification of a given event as signal or background was based on a discriminating variable \mathcal{D} . The discriminant \mathcal{D} was calculated from the signal (ρ_s) and the background (ρ_b) probability densities in the 6-dimensional vicinity of the event to be classified: $\mathcal{D} = \rho_s/(\rho_s + \rho_b)$. The probability densities were sampled with MC simulations and were calculated using a fast range-search algorithm. An inclusive CC DIS Monte Carlo simulation was used as background and a simulation of W^\pm -boson production as signal process.

Fig. 4a shows the shape of the resulting discriminant \mathcal{D} for data and simulations. The background (signal) is mostly located at low (large) \mathcal{D} values. The shape of the measured discriminant distribution is well described by the simulation. When applying a cut at $\mathcal{D} > 0.95$, a signal efficiency of $\epsilon_{\text{sig}} = 31 \pm 0.2\%$ and a background rejection $R = 1/\epsilon_{\text{bgd}} = 179 \pm 6$ were obtained. If in addition jets with only one track were required, the signal efficiency was $\epsilon_{\text{sig}} = 22 \pm 0.2\%$ and the background rejection improved to $R = 637 \pm 41$. With this cut value for the discriminant, an optimal separation between signal and background, $S = \sqrt{R} \cdot \epsilon_{\text{sig}}$, was obtained. Two alternative models were used to simulate the QCD cascade in the CC DIS simulation. The results from above were independent of the model choice. Using a NC DIS data sample, the probability to misidentify an electron^j or a jet with one track as tau lepton was determined to be on the permille level²⁶. The MC

^eThe event selection was mainly based on the requirement of large P_T^{miss} . Details can be found elsewhere²².

^fProbability Density Estimation based on Range Searching.

^gIn general, the internal jet structure is well modelled by the MC simulations²⁴.

^hJets were defined using the inclusive longitudinally invariant k_T algorithm¹⁸, $E_T > 5$ GeV and $-1 < \eta < 2.5$ was required.

ⁱThe subjet multiplicity describes the number of localised energy depositions within a jet that can be resolved using a certain resolution criterion. An exact definition can be found elsewhere^{24,25}.

^jTo reject electrons, additional cuts based on the electromagnetic energy fraction and the energy-momentum ratio were applied.

8 *T. Carli, D. Dannheim, L. Bellagamba*

simulations predicted the same misidentification probabilities.

In Fig. 4b the absolute number of measured and expected events is shown. To make the region of large \mathcal{D} values more visible, the x -axis was stretched according to $-\log(1 - \mathcal{D})$. For this inclusive CC event control selection, good agreement between data and simulation was found. However, at the largest \mathcal{D} values, slightly more events were found than expected by the SM processes.

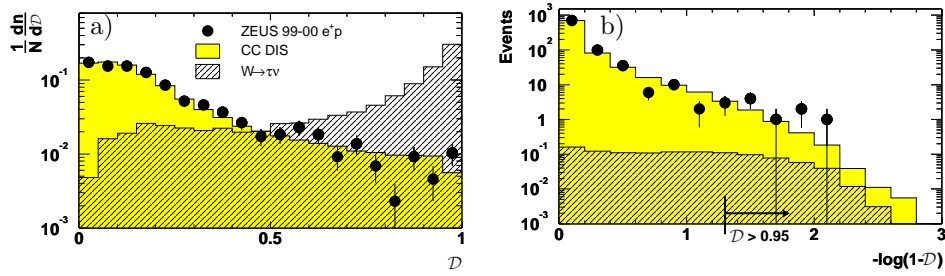


Fig. 4. Distribution of the tau-lepton discriminant, \mathcal{D} , for an inclusive selection of CC DIS data events (dots), a simulation of CC DIS events (shaded histograms) and the simulation of the W^\pm -boson production signal, where the tau lepton decays hadronically (hatched histograms). In each event, only the jet with the highest \mathcal{D} value enters. The histograms are normalised (a) to the total number of events N and (b) to the luminosity of the data. In (b), the $-\log(1 - \mathcal{D})$ distribution is displayed to expand the region in which the tau-lepton signal is expected.

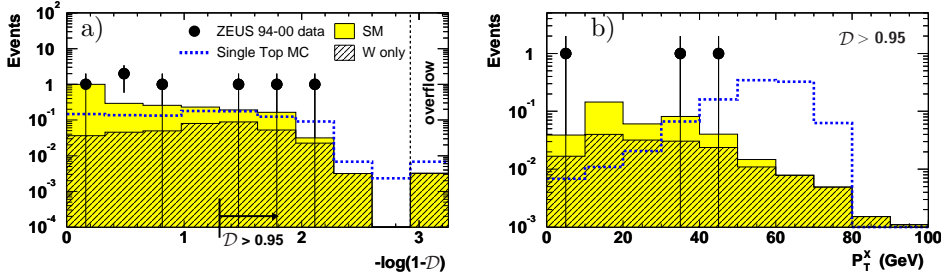


Fig. 5. Distribution of (a) the tau-lepton discriminant, $-\log(1 - \mathcal{D})$, before applying the cut $\mathcal{D} > 0.95$ and (b) the hadronic transverse momentum, P_T^X , after applying the cut $\mathcal{D} > 0.95$. The data (points) are compared to the SM expectations (shaded histogram). The hatched histogram shows the contribution of W^\pm -boson production. The dashed line shows a possible contribution of anomalous single top-quark production, normalised to an integral of one event.

4.2. Event Selection and Results

The event selection closely followed the ZEUS electron/muon analysis. The isolated track had to be associated to a tau-lepton candidate jet. To remove background from CC DIS, the jet-isolation requirement was tightened to $D_{jet} > 1.8$. The final

cut on P_T^X , optimised for the detection of tau-leptons originating from the decay of a heavy state, was set to $P_T^X > 25$ GeV. Seven events were found in the data, while only 2.2 ± 0.5 were expected from SM processes. Three events passed the cut $\mathcal{D} > 0.95$ (see Fig. 5a).

For $P_T^X > 25$ GeV ($P_T^X > 40$ GeV) two (one) events were found in the data and only 0.2 ± 0.05 (0.07 ± 0.02) events were expected from SM processes (see Fig. 5b). One of the data events at large P_T^X is shown in Fig. 6. The SM expectation was dominated by W^\pm -boson production. The Poisson probability to observe two or more events when 0.2 ± 0.05 are expected is 1.8%.

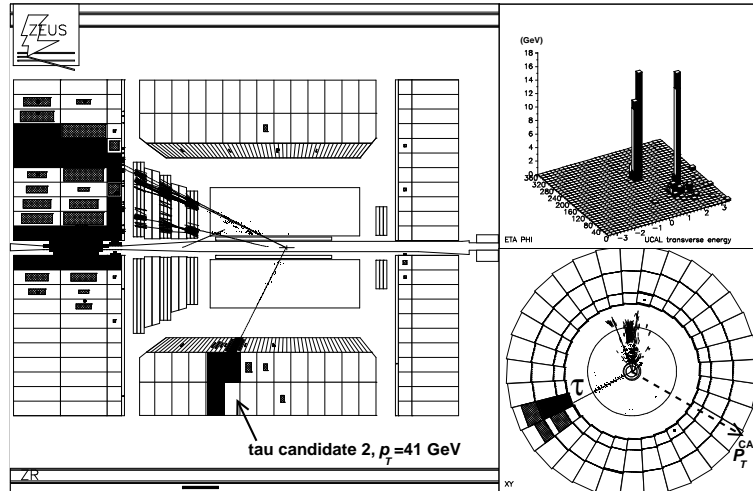


Fig. 6. Display of an isolated tau-lepton event with $P_T^{\text{miss}} = 39$ GeV and $P_T^X = 38$ GeV in the ZEUS detector.

5. Search for W^\pm Bosons in the Hadronic Decay Channel

Searches for events where the W^\pm boson decays hadronically were also performed^{3,4,6}. However, in this channel the SM backgrounds were so high that no firm conclusions could be drawn. In the H1 as well as in the ZEUS analysis the measured events were in agreement with the SM expectation dominated by QCD processes such as $\gamma p \rightarrow \text{jet jet}$. Anyway, since the sensitivity in the hadronic channel was lower than in the leptonic channel, the H1 excess in the leptonic channel is not contradicted by this result.

6. Interpretations Beyond the Standard Model

Several interpretations based on BSM effects have been proposed to explain the excess of events in the electron and muon channel measured by H1. The excess in

the tau-lepton channel recently reported by ZEUS has not yet been discussed.

6.1. Anomalous Single Top-Quark Production

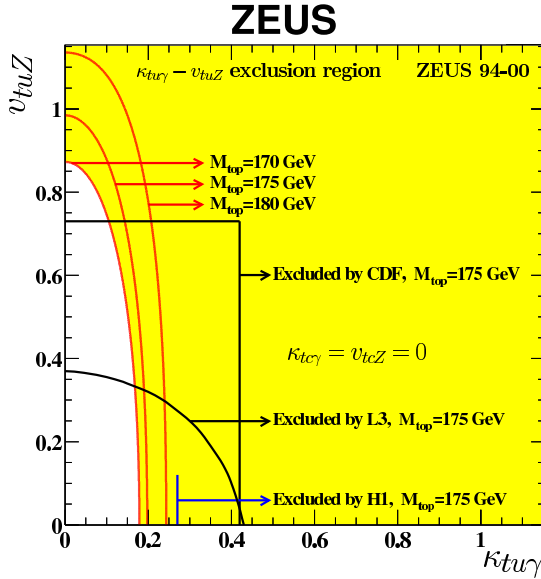


Fig. 7. Exclusion regions at 95% CL in the $\kappa_{tu\gamma} - v_{tuZ}$ plane for three values of M_{top} assuming $\kappa_{tc\gamma} = v_{tcZ} = 0$. The CDF and L3 exclusion limits are also shown.

lead to an enhancement of top production via FCNC couplings mediated by κ_{tqV} couplings (with $V = \gamma, Z^0$ and $q = u, c$). In order to evaluate the experimental sensitivity to FCNC single top-quark production, a magnetic coupling $\kappa_{tq\gamma}$ and a vector coupling v_{tuZ^0} are usually considered^{9,30}. Such couplings would induce the NC reaction $ep \rightarrow etX$ ^{9,31}, in which the incoming lepton exchanges a γ or Z^0 with an up-type quark in the proton^k.

ZEUS observed no event which is compatible with anomalous single top-quark production. H1 performed a dedicated analysis⁴ where the selection cuts were optimised for single top-quark events. Five events were observed, while 1.3 ± 0.2 were expected from SM processes. Since no significant excess was observed, both collaborations set limits on the coupling $\kappa_{tu\gamma}$ at 95% confidence level (CL), evaluated assuming $v_{tuZ} = 0$:

$$\kappa_{tu\gamma} < 0.27 \text{ (H1)} \quad \kappa_{tu\gamma} < 0.174 \text{ (ZEUS)}. \quad (1)$$

^kDue to the large Z^0 -mass the coupling to the photon is dominant at HERA. Moreover, a large value of the proton momentum fraction x is needed to produce the heavy top quark. Therefore, since the proton structure function at high x is dominated by valence quarks, HERA is only sensitive to couplings involving a u quark.

The production of a single heavy particle, like a top-quark decaying through the decay chain $t \rightarrow bW$, would naturally lead to the observed event topology. Within the SM, single top-quark production at the tree level can only proceed via a CC reaction $ep \rightarrow \nu t b X$ ²⁷, which, at HERA energies, has a cross section of less than 1 fb ²⁸, preventing any detection with the present integrated luminosity. Quark flavour changing neutral current (FCNC) processes are present only via higher order radiative corrections and are highly suppressed due to the Glashow-Iliopoulos-Maiani (GIM) mechanism²⁹. However, many extensions of the SM can

To extract these limits also the results on hadronic W^\pm -boson decay and NLO QCD corrections to the single top-quark cross section³¹ were included. The ZEUS collaboration also considered the effect of a non vanishing v_{tuZ} coupling. In this case a LO cross section, evaluated using the program CompHEP³², was used, since NLO corrections are not available for the full process. The H1 limit is less stringent because of the excess above the SM expectation observed in the electron and muon channels.

Fig. 7 shows the 95% CL ZEUS and H1 limits in the $\kappa_{tu\gamma}$ - v_{tuZ} plane, together with the results of the L3 collaboration³³ obtained in e^+e^- collisions at LEP³⁴ (the results of the other LEP collaborations are similar¹) and of the CDF collaboration³⁵ obtained in $p\bar{p}$ collisions at Tevatron. The limits were reported using HERA conventions for the couplings and assuming vanishing couplings to c -quarks. The HERA limits are the most stringent in the region of low v_{tuZ} . Due to the larger sensitivity to the Z^0 -exchange process, the LEP experiments obtained the most stringent limits at large v_{tuZ} .

6.2. *R-Parity-Violating Supersymmetry*

Supersymmetry (SUSY) linking bosons and fermions provides a consistent framework for the unification of the gauge interactions (GUT). Assuming supersymmetric partners for SM particles, bosonic partners for fermions and vice-versa, it cures the radiative quadratic divergences to the Higgs boson mass stabilizing the gap between the GUT and the electroweak scale³⁶.

In the minimal SUSY extension of the SM, R -parity is a multiplicative quantum number which is $R_p = 1$ for SM particles and $R_p = -1$ for their SUSY partners^m. In R_p -conserving processes, SUSY particles are pair produced and the lightest SUSY particle (LSP) is stable. However, the most general renormalizable and gauge invariant SUSY Lagrangian contains R_p -violating (\mathcal{R}_p) terms³⁷ that allow for single SUSY-particle production and LSP decay into SM particles.

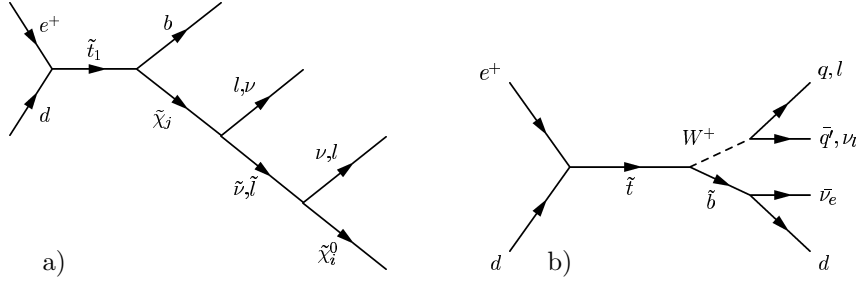
Of special interest for HERA are \mathcal{R}_p Yukawa couplings that couple a squarkⁿ to a lepton and a quark, allowing for resonant production of squarks through eq fusion³⁸. Such interactions are described in the SUSY Lagrangian by the term $\lambda'_{ijk} L^i Q^j \bar{D}^k$, where λ' is a Yukawa coupling, i, j and k are generation indices, L and Q denote the left-handed lepton and quark-doublet superfields and \bar{D} denotes the right-handed quark-singlet chiral superfield.

The coupling λ'_{1j1} gives rise to the reaction $e^+d \rightarrow \tilde{u}_L^j$ and the coupling λ'_{11k}

¹The Lagrangian used by the HERA and LEP experiments differs for a constant factor that leads to the following relations for the couplings $\kappa_{tu\gamma}^{\text{LEP}} = \sqrt{2} \cdot \kappa_{tu\gamma}^{\text{HERA}}$ and $v_{tuZ}^{\text{LEP}} = \sqrt{2} \cdot v_{tuZ}^{\text{HERA}}$. and Tevatron, differently from the HERA experiments, had similar sensitivity to both u - and c -quarks.

^m R -parity is defined as $R_p = (-1)^{3B+L+2J}$, where B is the baryon number, L the lepton number and J the spin of the particles.

ⁿThe SUSY partners of the fermions are in the following called squarks, sleptons etc., the ones of the bosons neutralino, photino, gluino etc.. SUSY particles are denoted by a tilde.

12 *T. Carli, D. Dannheim, L. Bellagamba*Fig. 8. Example Feynman diagrams for R_p -violating resonant squark production at HERA.

to $e^-u \rightarrow \tilde{d}_R^k$. The λ'_{131} coupling is of special interest since the large top mass implies a large mixing between the left- (\tilde{t}_L) and right-handed (\tilde{t}_R) states of the stop³⁹. As a consequence, the two stop mass eigenstates (\tilde{t}_1 and \tilde{t}_2) are strongly non-degenerate and \tilde{t}_1 is the best candidate to be the lightest squark. If the mass of \tilde{t}_1 is less than \sqrt{s} , the lighter stop can be resonantly produced via the λ'_{131} coupling and subsequently decay via R_p or gauge couplings.

Due to the large top-quark mass, scenarios exist where the two-body gauge decay modes involving a final-state top ($\tilde{t}_1 \rightarrow t\tilde{\chi}_i^0, t\tilde{g}$, where $\tilde{\chi}_i^0, i = 1..4$, and \tilde{g} are neutralinos and gluinos, respectively) are kinematically forbidden. In these scenarios high- P_T isolated leptons and large P_T^{miss} can be produced, as shown in Fig. 8a, through the decay chain $\tilde{t}_1 \rightarrow b\tilde{\chi}_j^+, \tilde{\chi}_j^+ \rightarrow \ell\tilde{\nu}_\ell(\nu_\ell\tilde{\ell}), \tilde{\ell}(\tilde{\nu}_\ell) \rightarrow \ell(\nu_\ell)\tilde{\chi}_i^0$ where $\tilde{\chi}_j^+$ ($j = 1, 2$) are charginos, $\ell(\nu_\ell)$ and $\tilde{\ell}(\tilde{\nu}_\ell)$ indicate a charged lepton (neutrino) and its supersymmetric partner, respectively^{8,40}. The charginos can be real or virtual (depending on the \tilde{t}_1 and $\tilde{\chi}_j^+$ mass difference) and the final state $\tilde{\chi}_i^0$ will decay to SM particles via an R_p coupling.

The exact process topology crucially depends on the SUSY parameters involved and on the relative strength between R_p and gauge couplings. At large values of $\tan\beta$, the ratio of the vacuum expectation value of the two neutral Higgs fields, the mixing between left- and right-handed states becomes relevant also in the τ sector leading to a light mass state $\tilde{\tau}_1$ and to an enhancement of tau-lepton production with respect to e and μ ⁴⁰. Considering the ZEUS excess in the isolated tau-lepton analysis⁷, it would be interesting to study this large $\tan\beta$ region of the SUSY parameter space in further detail.

An anomalous W^\pm -boson production can be caused by the other stop decay chain $\tilde{t}_1 \rightarrow \tilde{b}_1 W$, where \tilde{b}_1 , the lighter sbottom quark, can subsequently decay to $\tilde{b}_1 \rightarrow \bar{\nu}_e d$ via the λ_{131} coupling⁸. A diagram of this process is shown in Fig. 8b. The leptonic decay of the W^\pm boson would then lead to a high- P_T charged lepton in the final state. Such a process can be dominant only in a SUSY scenario where the \tilde{b}_1 is substantially lighter than the \tilde{t}_1 .

A dedicated search for squarks in R_p SUSY has been performed by H1⁴² including also the study of final states with electrons or muons, multi-jets and P_T^{miss} . No excess above SM expectation has been observed in this case.

6.3. Heavy Majorana Neutrinos

The recent observation of non-vanishing neutrino (ν) masses¹ might indicate the existence of heavy neutrino states. In most BSM scenarios, these new states are Majorana particles (N) and are very massive, i.e. $M_N \approx 10^2 - 10^{18}$ GeV, since they are related to the light neutrinos via the see-saw mechanism⁴¹.

At HERA, Majorana neutrinos could be directly produced^{43,44,45} via the reaction $e^+q \rightarrow Nq'$. In this case N is relatively light ($M_N < \sqrt{s}$) and decays via $N \rightarrow W^\pm e^\mp$. The Majorana neutrino could also be exchanged in the t -channel¹⁰, i.e. a W^\pm boson is emitted from the electron beam and fuses with a W^\pm boson from the proton beam: $e^+p \rightarrow W\bar{N}W \rightarrow \bar{\nu}_e l_1^+ l_2^+ X$, where l_1^+ and l_2^+ are two positively^o charged leptons which can have all lepton flavours. In this case M_N can be much bigger than \sqrt{s} . Since one of the two leptons has a sizeable probability not to be measured in the detector, the event topology would roughly fit to the experimental observation. In the direct production as well as in the t -channel exchange also dilepton events with large P_T^{miss} should be observable. This could allow to distinguish this production mechanism from other possibilities. A higher event rate is expected in e^-p collisions.

The size of the coupling depends on the angle mixing the light ν -state with N . However, for couplings not excluded by low energy experiments⁴⁶ and for reasonable values of $M_N \lesssim 1000$ GeV, the expected cross section is tiny^p. For the isolated electron and muon analyses only about $10^{-7} - 10^{-8}$ events are expected for the present integrated luminosities. The interest in this channel arises from the special role of the coupling of leptons belonging to the third generation, since limits on the mixing angles of third generation leptons are a factor of five weaker than for the first and second generation⁴⁷. Moreover, the production with two distinct lepton flavours leading to different final states is enhanced by a factor of about 3 with respect to the case with the same lepton flavours.

7. Consistency and Generic Interpretation of the Measurements

The H1 experiment observed 6 events with $P_T^X > 40$ GeV in the electron and muon channel while only 1.3 ± 0.3 events were expected from SM processes. The Poisson probability for the SM expectation to fluctuate to this observed number of events or more is 0.3%, corresponding to a significance of 2.8 standard deviations (σ)^q. The ZEUS results are in good agreement with the SM. However, ZEUS observed 2 events $P_T^X > 25$ GeV in the tau-lepton channel, where only 0.2 ± 0.05 events were expected, corresponding to an excess of approximately 2σ . So far, H1 has not released results in the tau-lepton channel.

^oThe leptons have the same charge sign as the incoming beam lepton.

^pNote, however, that the bounds from low energy experiments are model dependent⁴³.

^qThe number of standard deviations, σ , were obtained by relating the probability values to the case of a one-dimensional Gaussian distribution, such that the probability for a point to lie outside the quoted number of σ to one side of the mean is given.

Monte Carlo simulations were performed to evaluate whether the event yields, observed by the two experiments in the different channels, are compatible within SM background expectations or whether hypothetical BSM processes can lead to a more consistent interpretation²². In the following, three possible BSM scenarios are considered. Each scenario was characterized by an additional cross section, σ_{BSM} , leading to an extra-production of isolated leptons. A large number of randomly simulated experiments have been generated for each experimental result. Each simulated experiment was characterized by a number of observed events, $N_{\text{obs}}^{\text{MC}}$, generated from a Poissonian distribution with expectation value given by the sum of the SM expectation and the BSM contribution. The compatibility between the experimental results and the BSM scenario considered was studied varying σ_{BSM} and was measured by the variable $P_{\text{obs}}(\sigma_{\text{BSM}})$, defined as the fraction of randomly simulated experiments, which had a lower Poisson probability than the actual observation. The uncertainty in the SM expectation was taken into account in evaluating the Poisson probabilities.

In the following, anomalous production of W^\pm bosons, single top-quark production and anomalous production of tau leptons are considered as generic models for signal processes resulting in final states with isolated leptons (see Fig. 9).

7.1. Anomalous W^\pm -Boson Production

An anomalous W^\pm -production signal process with cross section $\sigma_{\text{W,BSM}}$ would, via a subsequent leptonic decay of the W^\pm boson, lead to events with isolated electrons, muons or tau leptons, as sketched in Fig. 9a. The detection efficiency for such a process was estimated from the efficiency for detecting SM W^\pm -boson production. Figure 10a shows the values of P_{obs} for the individual channels as a function of the hypothetical cross section $\sigma_{\text{W,BSM}}$. The maxima of the curves correspond to the most probable cross sections. For the ZEUS electron/muon channel, where no events were observed, the highest probability was obtained for no additional W^\pm -boson production cross section ($\sigma_{\text{W,BSM}} = 0$), while the H1 electron/muon analysis reached the largest value of P_{obs} for a cross section of $\sigma_{\text{W,BSM}} \approx 6$ pb. Due to the reduced efficiency in the ZEUS tau-lepton channel, it is most compatible with an even higher cross section of $\sigma_{\text{W,BSM}} \approx 23$ pb. The probabilities of all possible combinations of the three search channels are shown in Fig. 10b. The values for the most probable cross sections lie in between the ones for the individual channels. For the combination of all search channels, a value of $\sigma_{\text{W,BSM}} = 2.8$ pb has the highest probability of $P_{\text{obs}} = 0.6\%$. This still very low joint probability indicates that the set of observations hardly can be an outcome of the considered scenario. The probability assuming no additional cross section had a value of approximately $P_{\text{obs}} = 0.03\%$, corresponding to 3.4σ significance for a deviation from the SM.

7.2. Anomalous Single Top-Quark Production

A more specific model assumption on the anomalous W^\pm -boson production mechanism was made by comparing the observed event yields to the prediction from single top-quark production with cross section $\sigma_{\text{sing.top}}$. In case of H1, the results from the dedicated search for single top-quark production⁴ were considered, where five events were found while 1.3 ± 0.2 events were expected from SM background. The efficiency for single top-quark production in the ZEUS tau-lepton channel was approximately 25 times lower than in both the H1 and ZEUS combined electron/muon channels. Figure 10c and Fig. 10d show the values of P_{obs} for the individual search channels and for all combinations as a function of $\sigma_{\text{sing.top}}$. As expected from the low efficiency, the most probable cross section for the ZEUS tau-lepton channel reached a very large value of $\sigma_{\text{sing.top}} = 5$ pb. The combination of the ZEUS and H1 electron/muon channels alone, on the other hand, obtained a higher value for the maximum of $P_{\text{obs}} = 6\%$, since the H1 excess was lower in the dedicated single-top quark search compared to the generic search for isolated leptons. For the combination of all search channels, a value of $\sigma_{W,\text{BSM}} = 0.2$ pb had the highest probability of $P_{\text{obs}} = 0.6\%$. The probability assuming no additional cross section had a value of 0.1%, corresponding to approximately 3σ significance.

7.3. Anomalous Tau-Lepton Production

Anomalous direct production of tau-leptons in a process beyond the SM, e.g. as considered in section 6.2, could be the cause of both, the two tau-lepton events observed in the ZEUS tau-lepton search and the excess of electron and muon events in the H1 analysis. In this scenario, the tau-leptons do not originate from W^\pm -boson decays and hence the expected signal in the electron/muon channels consists only of leptonic tau-lepton decays. Assuming that the selection efficiency for those electrons and muons would be identical to the one for electrons and muons from SM single W^\pm -boson production, the efficiency (including the branching ratio) to identify tau-leptons in the hadronic channel was approximately the same as in the combined electron/muon channels. Figure 10e and Fig. 10f show the values of P_{obs} for the individual search channels and for all combinations as function of an anomalous tau-lepton production cross section $\sigma_{\tau,\text{BSM}}$. The probabilities assuming no additional cross section were identical to the ones from the first scenario (anomalous W -boson production), since the same observations and background expectations were considered. The combination of all search channels had a value of 0.03%. The most probable cross section value of $\sigma_{\tau,\text{BSM}} = 1.5$ pb corresponds to two expected signal events in the ZEUS tau-lepton channel as well as in the H1 and ZEUS combined electron/muon channels. The probability of 5% is higher than for the other cases. All results would be compatible on a level of better than two standard deviations. Therefore an anomalous tau-lepton production process could provide a more consistent interpretation of all measurements than the other scenarios considered.

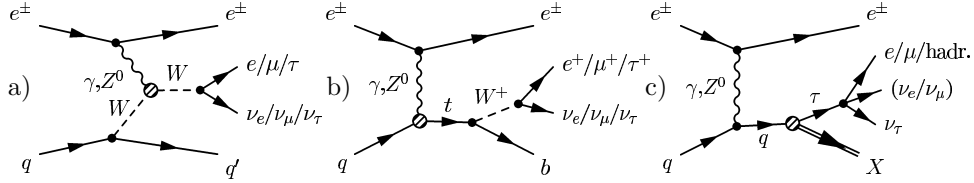
16 *T. Carli, D. Dannheim, L. Bellagamba*

Fig. 9. Diagrams for generic BSM processes which could lead to final states with isolated leptons: Anomalous W^\pm -boson production (a), single top-quark production (b) and anomalous tau-lepton production (c).

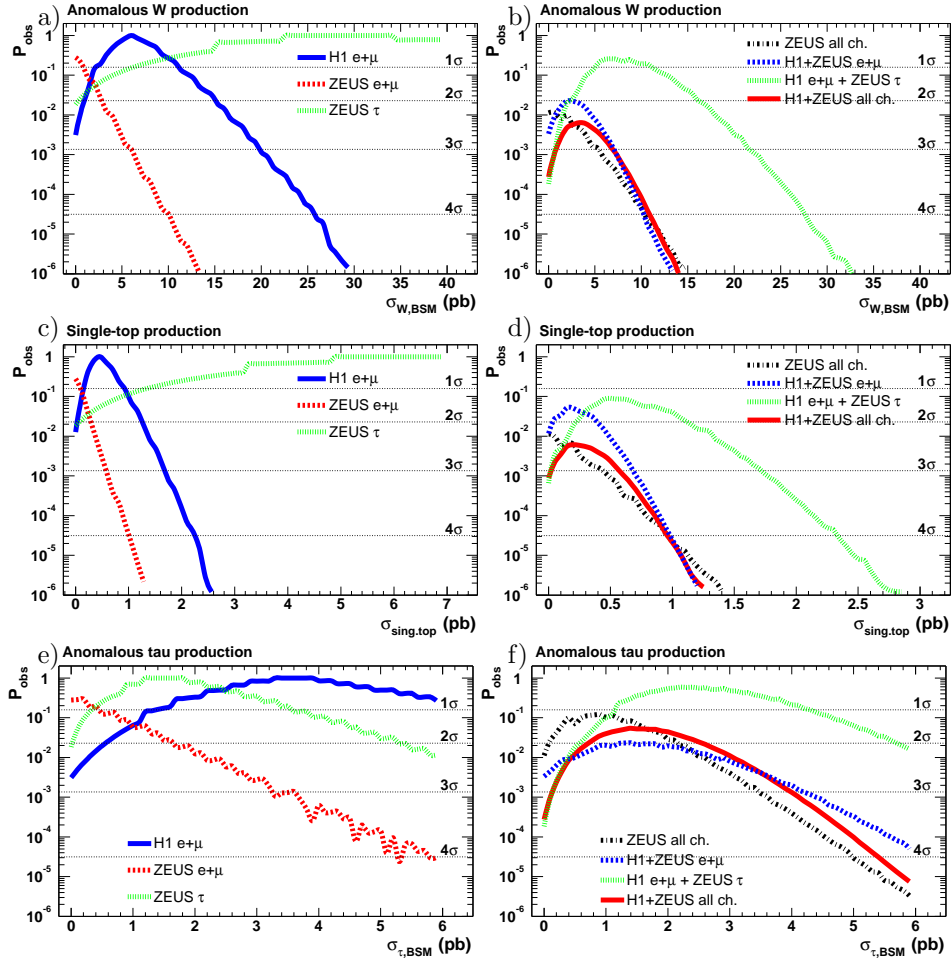


Fig. 10. Probabilities of the observed events yields, P_{obs} , for all combinations of the H1 and ZEUS search channels, as function of additional hypothetical cross sections for three generic BSM processes: anomalous production of W^\pm -bosons, single top quarks and tau-leptons. The fluctuations in the curves are caused by discontinuities of the Poisson probabilities, which were calculated for discrete event numbers.

8. Outlook

8.1. Isolated Lepton Events

The high luminosity expected for the HERA-II data taking period can help to clarify whether the excess of measured events in the electron, muon and tau-lepton channels over the SM expectation were due to a statistical fluctuation or to a new BSM interaction. Figure 11 compares different scenarios for the expected event

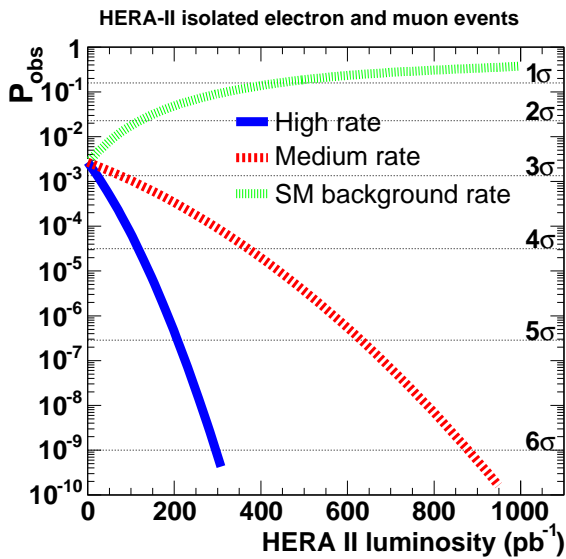


Fig. 11. Poisson probabilities of expected future event yields in the combined H1 and ZEUS isolated electron and muon searches of the future HERA-II data taking for three scenarios, as explained in the text.

was assumed that both experiments will observe events at a high rate, corresponding to the H1 rate in the 1994-2000 data taking periods. After an additional luminosity of 200 pb^{-1} , a deviation from the SM expectation with a significance of approximately 5σ will be observed in this case. The second scenario assumed that both experiments will observe events at the average of the previous H1 and ZEUS rates. In this case, the significance for a deviation from the SM will be about 3σ after an additional luminosity of 200 pb^{-1} , while after 600 pb^{-1} the significance will increase to approximately 5σ . In the third scenario, only the SM background rate will be observed in both experiments. In this case, the combined H1 and ZEUS results will reach agreement with the SM within $1 - 2\sigma$ after approximately 150 pb^{-1} . The sensitivity can be further increased, if the tau-lepton channel is also considered and if the improvements in both the H1 and ZEUS detectors are exploited.

yields in future H1 and ZEUS searches for isolated electron and muon events. It was assumed that the background rates and their uncertainties, scaled to the additional luminosity, and the signal efficiencies will be the same as in the 1994-2000 analyses. Different assumptions on the future event rates R_{fut} were made. The probability P_{obs} was defined as the fraction of simulated SM-background-rate experiments, which had a lower Poisson probability than the actual simulated observation with rate R_{fut} . The probabilities P_{obs} are displayed as a function of the additional HERA-II luminosity. In the first scenario it

8.2. Single Top-Quark Production

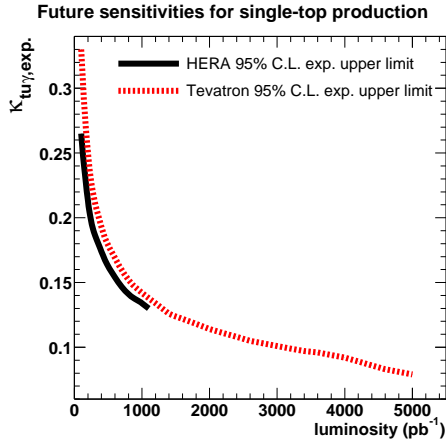


Fig. 12. Expected future sensitivities of the HERA and Tevatron searches for single top-quark production.

by scaling the background expectations to the additional luminosity expected from their Run-II. For an additional luminosity of 500 pb^{-1} , the HERA experiments will be sensitive down to a coupling strength of $\kappa_{tu\gamma} \lesssim 0.16$. The Tevatron experiments will have a similar sensitivity.

9. Conclusion

Both, the H1 and ZEUS collaborations observed more events with isolated leptons, large P_T^{miss} and large P_T^X than expected from the SM. While H1 observed an excess of approximately three standard deviations in the combined electron and muon channels, ZEUS saw agreement with the SM in these channels. In the tau-lepton channel, however, which has only been investigated by the ZEUS collaboration so far, two events were observed. This corresponds to an excess of approximately two standard deviations. The probability that these measurements are simultaneously realised in random experiments is 0.03%, i.e. a 3.4σ deviation from the SM expectation was observed. The deviation is large, however, the lack of agreement between the two experiments in the individual search channels complicates a consistent interpretation of the results.

Several models beyond the SM could explain an excess of isolated lepton events as originating from the decays of heavy states. For certain processes, like e.g. photon mediated anomalous single top-quark production, the HERA experiments have a higher sensitivity than any other collider. The addition of an anomalous production of single top-quarks or W^\pm -bosons does not significantly improve the consistency of the measurements. However, an anomalous production of tau leptons with a cross section of about 1 pb could, through the leptonic and hadronic decays, consistently

The future sensitivity of the HERA experiments for anomalous single top-quark production was estimated from a simulation of the expected event yields in the ZEUS single-top search, assuming that only background processes will be measured. The anomalous vector coupling to the Z^0 -boson, v_{tuZ} , was assumed to be vanishing and LO calculations for the single top-quark cross section were used in the simulations. Figure 12 shows the resulting expected 95% C.L. upper limit on the photon coupling, $\kappa_{tu\gamma}$, as a function of the additional HERA-II luminosity. For comparison, also the expected sensitivity of the Tevatron experiments is shown, estimated from the present CDF results³⁵

explain all the measurements. R_p SUSY models provide scenarios allowing for such a BSM tau-lepton production.

The HERA-II data taking period will help to clarify the origin of the observed excess of isolated lepton events, if an additional luminosity of $150\text{-}600\text{ pb}^{-1}$ can be accumulated. The sensitivity for anomalous single top-quark production will in this case improve to values of $\kappa_{t\tau\gamma} \lesssim 0.16$.

Acknowledgements

We would like to thank W. Buchmüller, C. Diaconu, E. Gallo, M. Kuze and F. Schrempp for critical reading of the manuscript and helpful comments.

References

1. Super-Kamiokande Coll., Y. Fukuda et al., Phys. Rev. Lett. 81 (1998) 1562; SNO Coll., Q.R. Ahmad et al., Phys. Rev. Lett. 87 (2001) 071201; KamLAND Coll., Phys. Rev. Lett. 90 (2003) 021802.
2. M. Kuze and Y. Sirois, Prog. Part. Nucl. Phys. 50 (2003) 1.
3. H1 Coll., V. Andreev et al., Phys. Lett. B 561 (2003) 241.
4. H1 Coll., V. Andreev et al., DESY report 03-132 (2003), accepted by Eur. Phys. J.; <http://www-h1.desy.de/h1/www/publications/htmlsplit/DESY-02-224.long.html>
5. ZEUS Coll., J. Breitweg et al., Phys. Lett. B 471 (2000) 411.
6. ZEUS Coll., S. Chekanov et al., Phys. Lett. B 559 (2003) 153; addendum in: DESY report 03-188 (2003).
7. ZEUS Coll., S. Chekanov et al., DESY report 03-182 (2003), accepted by Phys. Lett. B.
8. T. Kon, T. Kobayashi and S. Kitamura, Phys. Lett. B 376 (1996) 227; T. Kon, T. Kobayashi, S. Kitamura and T. Iimura, Phys. Lett. B 494 (2000) 280; T. Kon and T. Kobayashi, Phys. Lett. B 409 (1987) 265.
9. H. Fritzsch and D. Holtmannspötter, Phys. Lett. B 457 (1999) 186.
10. W. Rodejohann and K. Zuber, Phys. Rev. D 62 (2000) 094017.
11. U. Baur and D. Zeppenfeld, Nucl. Phys. B 325 (1989) 253.
12. L3 Coll., M. Acciarri et al., Phys. Lett. B 467 (1999) 171; ALEPH Coll., A. Heister et al., Eur. Phys. J. C 21 (2001) 423; OPAL Coll., G. Abbiendi et al., CERN-EP-2003-042, Jul 2003, hep-ex/0308067; DELPHI Coll., P. Abreu et al., Phys. Lett. B 423 (1998) 194; and references therein.
13. D0 Coll., B. Abbott et al., Phys. Rev. D 62 (2000) 052005; CDF Coll., Phys. Rev. Lett. 78 (1997) 4536; and references therein.
14. U. Baur, J.A.M. Vermaseren and D. Zeppenfeld, Nucl. Phys. B 375 (1992) 3.
15. C. Diaconu, in: Workshop on Monte Carlo Generator for HERA Physics, ed. A. Doyle et al., DESY-PROC-1999-02, p. 631.
16. K.P. Diener, C. Schwanenberger and M. Spira, Eur. Phys. J. C 25 (2002) 405; see also: P. Nason, R. Rückl and M. Spira, J. Phys. G 25 (1999) 1434; M. Spira, Preprint DESY-99-060, hep-ph/9905469 (1999).
17. K.P. Diener, C. Schwanenberger and M. Spira, Preprint hep-ex/0302040 (2003).
18. S. D. Ellis and D. E. Soper, Phys. Rev. D 48 (1993) 3160; S. Catani et al., Nucl. Phys. B 406 (1993) 187.
19. H1 Coll., T. Ahmed et al., DESY report 94-248 (1994).
20. H1 Coll., C. Adloff et al., Eur. Phys. J. C 5 (1998) 575.

20 *T. Carli, D. Dannheim, L. Bellagamba*

21. H1 Coll., S. Aid et al., *Z. Phys. C* 71 (1996) 211.
22. D. Dannheim, PhD-thesis, Univ. Hamburg, Report DESY-THESIS-2003-025, 2003.
23. T. Carli and B. Koblitz, *Nucl. Inst. Meth. A* 501 (2003) 576.
24. H1 Coll., C. Adloff et al., *Nucl. Phys. B* 545 (1999) 3; ZEUS Coll., S. Chekanov et al., *Phys. Lett. B* 558 (2003) 41.
25. J.R. Forshaw and M.H. Seymour, *JHEP* 09 (1999) 009; M.H. Seymour, *Nucl. Phys. B* 421 (1994) 545.
26. D. Lelas, PhD-thesis, Univ. Hamburg, in preparation.
27. G. Schuler, *Nucl. Phys. B* 299 (1988) 21; U. Baur and J.J. van der Bij, *Nucl. Phys. B* 304 (1988) 451; J.J. van der Bij and G.J. van Oldenborgh, *Z. Phys. C* 51 (1991) 477.
28. T. Stelzer, Z. Sullivan and S. Willenbrock, *Phys. Rev. D* 56 (1997) 5919; S. Moretti and K. Odagiri, *Phys. Rev. D* 57 (1998) 3040.
29. S.L. Glasho, J. Iliopoulos and L. Maiani, *Phys. Rev. D* 10 (1970), 1285.
30. H. Fritzsch, *Phys. Lett. B* 224 (1989) 423; R.D. Peccei and X. Zhang, *Nucl. Phys. B* 337 (1990) 269; T. Han, R.D. Peccei and X. Zhang, *Nucl. Phys. B* 454 (1995) 527; G.M. Divitiis, R. Petronzio and L. Silvestrini, *Nucl. Phys. B* 504 (1997) 45.
31. A. Belyaev and N. Kidonakis, *Phys. Rev. D* 65 (2002) 037501.
32. A. Pukhov et al., hep-ph/9908288.
33. L3 Coll., P. Achard et al., *Phys. Lett. B* 549 (2002) 290.
34. ALEPH Coll., R. Barate et al., *Phys. Lett. B* 494 (2000) 33; ALEPH Coll., A. Heister et al., *Phys. Lett. B* 543 (2002) 173; OPAL Coll., G. Abbiendi et al., *Phys. Lett. B* 521 (2001) 181.
35. CDF Coll., F. Abe et al., *Phys. Rev. Lett.* 80 (1998) 2525.
36. E. Witten, *Nucl. Phys. B* 188 (1981) 513.
37. S. Weinberg, *Phys. Rev. D* 26 (1982) 287; N. Sakai, T. Yanagida *Nucl. Phys. B* 197 (1982) 83; S. Dinopoulos, S. Raby, F. Wilczek, *Phys. Lett. B* 212 (1982) 133.
38. V. Barger, G.F. Giudice and T. Han, *Phys. Rev. D* 40 (1989) 2987; J. Butterworth and H. Dreiner, *Nucl. Phys. B* 397 (1993) 3.
39. J. Ellis and S. Rudaz, *Phys. Lett. B* 128 (1983) 248; G. Altarelli and R. Rückl, *Phys. Lett. B* 144 (1984) 126; I. Bigi and S. Rudaz, *Phys. Lett. B* 153 (1985) 335.
40. W. Porod, *Phys. Rev. D* 59 (1999) 095009.
41. R. N. Mohapatra and G. Senjanovic, *Phys. Rev. Lett.* 44 (1980) 912.
42. H1 Collab., C. Adloff et al., *Eur. Phys. J. C* 20 (2001) 639.
43. W. Buchmüller and C. Greub, *Nucl. Phys. B* 363 (1988) 345.
44. M. Flanz, W. Rodejohann and K. Zuber, *Phys. Lett. B* 373 (2000) 324; erratum *ibid.* B 480 (2000) 418.
45. G. Ingelman and J. Rathsman, *Z. Phys. C* 60 (1993) 243.
46. G. Belanger et al., *Phys. Rev. D* 53 (1996) 6292.
47. E. Nardi, E. Roulet and D. Tommasini, *Phys. Lett. B* 344 (1995) 225.